Influence of charge mobility on the equilibrium properties of polyelectrolytes in salt solutions: a Monte Carlo study

ARTICLE *in* MACROMOLECULES · DECEMBER 1993

Impact Factor: 5.8 · DOI: 10.1021/ma00077a024

3 AUTHORS, INCLUDING:

Dick Bedeaux
Norwegian University of Science and Technol…

305 PUBLICATIONS **5,477** CITATIONS

Influence of Charge Mobility on the Equilibrium Properties of Polyelectrolytes in Salt Solutions: A Monte Carlo Study

Th. M. A. O. M. Barenbrug, J. A. M. Smit, and D. Bedeaux*

Department of Physical and Macromolecular Chemistry, Gorlaeus Laboratories, Leiden University, P.O. Box 9502, 2300 RA Leiden, The Netherlands

Received June 24, 1993; Revised Manuscript Received September 29, 1993®

ABSTRACT: Using a Metropolis algorithm, various average properties of "lattice polyelectrolytes" were calculated, i.e. the squared end-to-end distance, the squared radius of gyration, the apparent persistence length, the charge distribution over the segments, the average distance between the charges and the center of mass, and the eccentricities of the mass and charge distributions. Lattice polyelectrolytes are self-avoiding random walks on a (3-dimensional) cubic lattice, bearing either equidistantly fixed or mobile, discrete charges. For the electrostatic interaction a Debye–Hückel potential is used. Differences due to charge mobility along the chain are analyzed. It is found that most of these differences can be explained in terms of a more uniform average charge distribution in the mobile case, and a charge accumulation of the mobile charges near the ends of the chain. Furthermore, the mobile charges will tend to preferentially localize themselves away from bends in the chain, thus enhancing its flexibility. Our results for the end-to-end distance and chain stiffness for increasing charge density are compared with the theoretical results given by Katchalsky, Odijk, Schmidt, Skolnick and Fixman, and also with (other) simulation results by Carnie, Christos, and Creamer.

1. Introduction

In the last decades much work has been done on the statistical and thermodynamic properties of polyelectrolytes; cf. the review by Mandel.[1] The repeating units of these polymers are charged (e.g. in the case of strong polyacids) or *may* be charged, as is the case in partially neutralized weak polyacids. As a result of the long range Coulombic repulsion, the statistical properties of such a system can, in general, not be evaluated analytically. This is due in particular to the presence of small, mobile ions in the solution (counterions of the polyanion and ions provided by added salt), which interact with the polyion and with each other. A possible way to describe these complex systems is by computer simulations. In order to make these simulations not too time-consuming it is usually assumed that the charged segments of the polyelectrolyte interact with each other through a potential of mean force, i.e. the force averaged with respect to the equilibrium distribution of the solvent and mobile ions. In this way the system is reduced to just the polyion segments and their interactions.[2,3] As the potential of mean force the Debye–Hückel potential is used, which is a good approximation, particularly for weakly charged polyelectrolytes.[2]

In most studies the charges of the polyions are assumed to be either positioned equidistantly on the polymer backbone[5–7,12] or to be spread continuously along the backbone, the polyelectrolyte thus forming a line charge.[4,8,9,12] Charge mobility along the backbone, which comes into play if one deals with partially charged, weak polyacids, and which gives rise to fluctuations in charge density on the chain and changes in the overall shape of the polyion, has hitherto not thoroughly been studied.[10–12] In this paper we consider cases of both mobile and fixed charges. In section 2 we treat the details of the model and the methods followed. In section 3 the MC results are given and briefly discussed. In section 4 we discuss some significant differences in the behavior, induced by the charge mobility, in more detail. In section 5 we compare our findings with some theoretical predictions for fixed charges.[4,12,16–19] In our analysis we consider polyions of 10, 20, 40, and 80 segments for which we calculate various properties: either by exact enumeration of the partition sums (in the case of short chains: $n \leq 10$), or by Monte Carlo methods (for longer chains), both for the mobile and for the equidistantly fixed charge distribution. Interactions between different polyions are ignored.

2. Model and Methods

The model polyelectrolyte consisting of $n+1$ segments, q of them charged with the elementary charge e, is represented by an n-step self-avoiding random walk (SAW) on a (3-dimensional) cubic lattice, a well-known way of modeling a polymer in a good solvent. The segments are given the overall length, a, of one monomer of the polyion. In our choice of parameters we use $a = 2.515 \times 10^{-10}$ m, which is appropriate for acrylic acid. One could argue, that 180 and 90° angles are not "natural" for this system. But as every segment contains two C–C bonds, any other angle is not "natural" either.[6] Besides, we expect that the essential relative differences due to the mobility of the charges will not depend too strongly on the symmetry of the lattice.[13] Every polyion conformation is represented by $\{\mathbf{r}_i, Q_i\}$ where the $\mathbf{r}_i$ describe the positions of the i segments ($i \in \{0, 1, ..., n\}$) and the Q_i are either 0 or 1, depending on the ith segment being charged or not in this particular conformation. In the fixed-charge case the q charges are positioned equidistantly (as far as possible) and their positions along the chain are kept fixed during the Monte Carlo simulation. In the mobile-charge case the charges are allowed to reside on any of the segments, and their positions along the chain are changed at each step of the Monte Carlo simulation. In the course of the calculation the total number of charges, q, is held fixed.

The charges are assumed to interact according to a Debye–Hückel potential, which is given as a function of the distance r by

$$\psi(r) = \frac{e e^{-\kappa r}}{4\pi\epsilon r} \qquad \text{where} \qquad \kappa^2 = \frac{1000 N_A e^2 C_0}{\epsilon k T} \tag{1}$$

in which κ is the reciprocal Debye screening length, N_A is the Avogadro number, e is the elementary charge, C_0 is the concentration of small ions present (in mol/L), ϵ is the dielectric constant of the solvent, k is the Boltzmann

* To whom correspondence should be addressed.

® Abstract published in *Advance ACS Abstracts*, November 1, 1993.

0024-9297/93/2226-6864$04.00/0

constant, and T is the absolute temperature (all quantities in SI units). The Debye–Hückel potential is most appropriate if the system contains only monovalent small ions.[23] The use of this potential makes the model in particular appropriate for weak polyelectrolytes.[2,4] Our analysis is less realistic for charge densities higher than about 35% (estimated for a line charge, with the chosen value of a), due to the phenomenon of counterion condensation.[8] The reason for considering in this paper also larger charge densities is to make a comparison with other theories and simulation data for these high charge densities.

The (total) energy, E, of a particular polyion conformation $\{\mathbf{r}_i,Q_i\}$ is taken as the sum over all pair interactions of the polyion charges.

$$\frac{E}{kT} = \sum_{i=0}^{n-1}\sum_{j=i+1}^{n} Q\frac{Q_iQ_j}{|\mathbf{r}_i - \mathbf{r}_j|}\exp\{-\kappa|\mathbf{r}_i - \mathbf{r}_j|\} \qquad (2)$$

where k is Boltzmann's constant and Q ($\equiv e^2/4\pi\epsilon kT$) is the Bjerrum length. Using these interaction energies and assuming a canonical distribution of conformations, one can compute quantities as for instance the mean square radius of gyration:

$$R_g^2 = \frac{1}{n+1}\langle\sum_{i=0}^{n}(\mathbf{r}_i - \mathbf{R}_{com})^2\rangle = \frac{1}{2(n+1)^2}\langle\sum_{j=0}^{n}\sum_{i=0}^{n}(\mathbf{r}_i - \mathbf{r}_j)^2\rangle \qquad (3)$$

in which $\langle ... \rangle$ represents the canonical ensemble average over all possible configurations of the polyion. As is clear from this expression, R_g^2 is equal to the mean square distance between the position of the segments and the center of mass ($\mathbf{R}_{com}$), and also to the mean square distance between all segments. In an analogous way we define the "charge radius of gyration", R_q^2, as being the mean square distance between the position of the charges and the center of mass:

$$R_q^2 = \frac{1}{q}\langle\sum_{i=0}^{n}Q_i(\mathbf{r}_i - \mathbf{R}_{com})^2\rangle \qquad \text{where} \qquad q = \sum_{i=0}^{n}Q_i \qquad (4)$$

Furthermore, the average squared end-to-end distance, R_e^2, is defined as the average squared length of the end-to-end vector, $(\mathbf{r}_n - \mathbf{r}_0)$, which connects the centers of the first and last segment

$$R_e^2 = \langle|\mathbf{r}_n - \mathbf{r}_0|^2\rangle \qquad (5)$$

Finally, the average projection of the end-to-end vector on the line connecting the first two segments is defined by (see ref 21, p 401)

$$L_t = \frac{1}{a}\langle(\mathbf{r}_n - \mathbf{r}_0)\cdot(\mathbf{r}_1 - \mathbf{r}_0)\rangle \qquad (6)$$

in which a (the lattice constant, equal to $|\mathbf{r}_1 - \mathbf{r}_0|$), is added as a normalizing factor. The quantity L_t will be interpreted as the length-(n)-dependent persistence length near the end of the chain. In the following we shall call this quantity the *apparent persistence length*.

For wormlike chains, L_t approaches in the large n limit the real persistence length, L_p, of the chain:

$$L_p \equiv \lim_{n\to\infty} L_t \qquad (7)$$

In principle one could define a *local* (position and length dependent) persistence length along the chain by a similar projection on each of the other bond vectors (see ref 15, page 111). In the fixed-charge case such a quantity would depend on the location of the charges relative to the chosen bond vector, and it would not be a convenient property to compare with the mobile-charge case. As the end segments are always charged (in the fixed-charge case), our definition of L_t enables a proper comparison. For the validity of eq 7 it would in fact be more appropriate to take the limit of some average of a position dependent persistence length. We will not investigate this point any further.

The persistence length may be written as the sum of an intrinsic, charge independent part L_0 and an electrostatic part L_e:

$$L_p = L_0 + L_e \qquad (8)$$

An explicit theoretical expression for L_e has been given by Odijk[4]—provided that the polyion is rodlike over the range of the electrostatic interaction: $\kappa L_p \geq 1$—and also by Skolnick and Fixman.[12] L_0 can be determined numerically as the persistence length of the uncharged chain, and one finds $L_0 \approx 1.42a$ for the cubic lattice.[13] L_e results from the presence of the charges.

If the positions of the charges along the chain are fixed and equidistant, the mass and the charge distributions of long polyions are expected to be very similar. For mobile charges this is no longer necessarily the case. It is therefore interesting to consider quantities which are indicative of such a difference, for instance the second moments of the mass distribution and of the charge distribution, relative to the center of mass. The second moment of the mass distribution is given by

$$M_{kl} \equiv \langle\sum_{i=0}^{n}(\mathbf{r}_i - \mathbf{R}_{com})_k(\mathbf{r}_i - \mathbf{R}_{com})_l\rangle \qquad (9)$$

The subscript k in $\mathbf{A}_k$ signifies the kth component of the vectorial quantity $\mathbf{A}$. In an analogous way the second moment of the charge distribution is given by

$$Q_{kl} \equiv \langle\sum_{i=0}^{n}Q_i(\mathbf{r}_i - \mathbf{R}_{com})_k(\mathbf{r}_i - \mathbf{R}_{com})_l\rangle \qquad (10)$$

For symmetry reasons, only the diagonal elements of the moments of both the mass and charge distribution are unequal to zero. Taking the first step of every conformation in the x-direction, gives, again for symmetry reasons: $M_{yy} = M_{zz}$ and $Q_{yy} = Q_{zz}$. M_{xx} compared to M_{yy} yields information about the relative stretching of the polyion itself, expressed by the mass eccentricity, e_m. The relative stretching of the charge distribution is expressed by a similar quantity: the charge eccentricity, e_q. Both are defined by

$$e_m^2 = 1 - \frac{M_{yy}}{M_{xx}} \qquad \text{and } e_q^2 = 1 - \frac{Q_{yy}}{Q_{xx}} \qquad (11)$$

Note that the former is non-zero for short chains, even at zero charge, because of the self-avoiding property of the chains. A comparison of the eccentricities of the mass and charge distributions reveals information about the spatial distribution of the charge over the segments.

Comparison of eqs 3, 4, 9, and 10 leads to

$$R_g^2 = M_{xx} + M_{yy} + M_{zz} = M_{xx} + 2M_{yy} \qquad (12)$$

and

$$R_q^2 = Q_{xx} + Q_{yy} + Q_{zz} = Q_{xx} + 2Q_{yy} \qquad (13)$$

In this paper we calculate the quantities introduced above for chain lengths up to 80 segments, various charge densities, and two different values of κa. The charges are taken as both mobile and fixed in the calculations. The

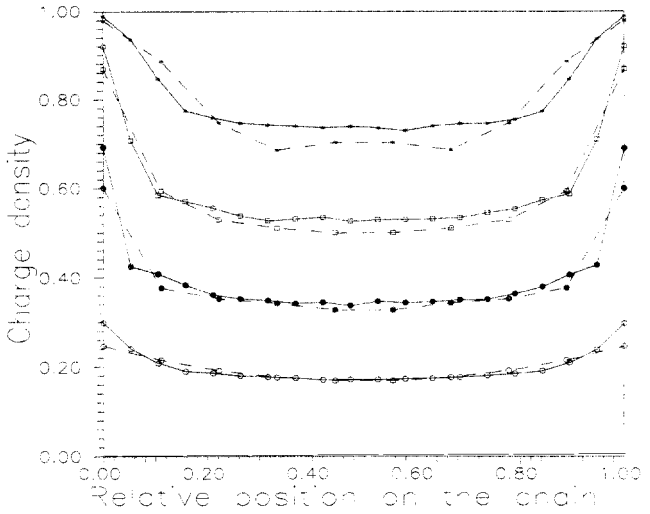

Figure 1. Average charge distributions of mobile charges along chains of 10 (- - -) and 20 (—) segments, for charge densities of 20% (○), 40% (●), 60% (□), and 80% (*), at $\kappa a = 0.1$.

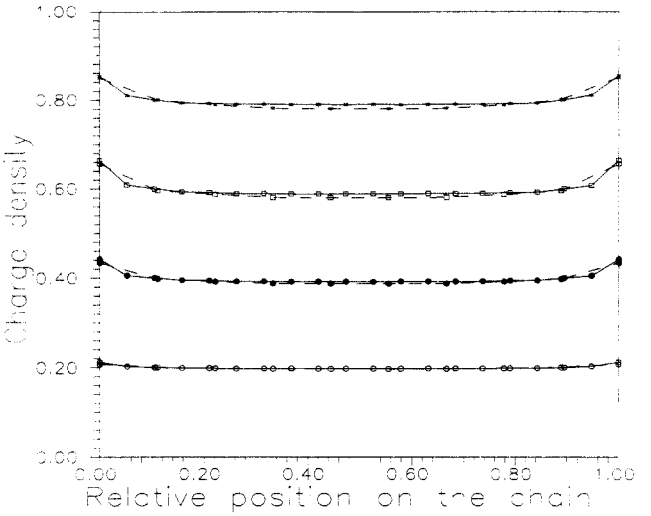

Figure 2. Average charge distributions of mobile charges along chains of 10 (- - -) and 20 (—) segments, for charge densities of 20% (○), 40% (●), 60% (□), and 80% (*), at $\kappa a = 2.0$.

averages of the quantities R_e^2, R_g^2, R_q^2, L_t, E, M_{kl}, Q_{kl}, described in eqs 2–6 and 9–11, and also the average charge distribution over the segments are computed either by exact enumeration of the partition sums and averages (for $n \leq 10$), or by a Monte Carlo algorithm according to Metropolis[14] for the longer chains.

The conformation space is sampled using a pivot algorithm,[15] which is an efficient way to generate SAW's on a cubic lattice, in particular for charged and therefore generally rather expanded conformations. For every step of the Metropolis algorithm a new spatial configuration as well as a new charge distribution (only in the mobile case!) is chosen at random. The transition probability of moving from a given configuration i with energy E_i to a random configuration j with energy E_j is given by

$$p(i \rightarrow j) = \frac{e^{(E_i - E_j)/kT}}{e^{(E_i - E_j)/kT} + 1} \qquad (14)$$

A simple way to realize these transition probabilities is by choosing a random number s between 0 and 1. This number decides whether this new configuration is chosen (if $s \leq \exp(E_i - E_j)$) or not (in case $s > \exp(E_i - E_j)$). The resulting configuration then provides the new quantities (given by (2)–(6), (9), and (10)) which are in this way automatically averaged in accordance to their relative importance. Using this algorithm for $n \leq 10$ we could reproduce the exact results within a relative error of 0.5%, after sampling 5.0×10^6 times, which is an indication of the correctness of the used algorithms. Averaging for the larger values of n took place until the estimated relative error in the results was smaller than 2% for chains up to $n = 40$ and smaller than 5% for $n = 80$.

3. Results of the MC Calculations

Results are presented for the various quantities defined above, for chains of 10, 20, 40, and 80 segments. As Bjerrum length we use 7.0×10^{-10} m, which corresponds to a temperature of 298 K. Furthermore we used $\epsilon = 78\epsilon_0$ as the dielectric constant of the solvent (water). ϵ_0 is the vacuum dielectric constant. In the figures all lengths are given in units of the lattice constant. (For acrylic acid: $a = 2.515 \times 10^{-10}$ m.)

In Figures 1 and 2 the charge distributions for mobile charges are plotted for various charge densities, for n = 10 and 20, for $\kappa a = 0.1$ and $\kappa a = 2.0$, respectively. It is found that the charge density along the chain has maxima near the ends of the chain and becomes more or less constant, in particular for longer chains, around the middle part of the chain. For $\kappa a = 0.1$, the charge density away from the end points is on the order of 10% below the (overall) average charge density. For $\kappa a = 2.0$ the effect of charge accumulation near the end points is, though still present, much less important, due to the strong Debye screening. In this case the charge density away from the end points is only on the order of 1% below the average charge density.

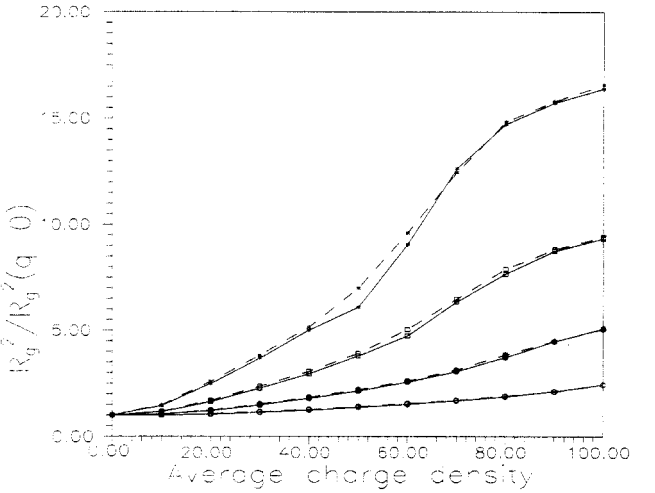

Figure 3. Normalized squared radius of gyration: $R_g^2/R_g^2(q=0)$, versus the average charge density, for chains of 10 (○), 20 (●), 40 (□), and 80 (*) segments, either with mobile (—) or equidistantly fixed (- - -) charges. $\kappa a = 0.1$.

In Figure 3 the squared radius of gyration, R_g^2, is plotted as a function of the average charge density, for $\kappa a = 0.1$ and for n = 10, 20, 40, and 80. This is done for both mobile and fixed charges. It is found, that for longer chains and for a charge density of about 50%, the $R_{g,\text{mobile}}$ becomes somewhat smaller than $R_{g,\text{fixed}}$. This is a consequence of the mobility of the charges, as the charges will tend to preferentially localize themselves away from bends in the chain. This increases the flexibility, as compared to the chain with fixed charges. As is to be expected, this effect is most predominant for a charge density which is neither too high (in that case the mobility is rather limited) nor too low, when the fixed-charge chain is also rather flexible.

In Figure 4 the squared "charge radius of gyration", R_q^2, is plotted as a function of the average charge density, for

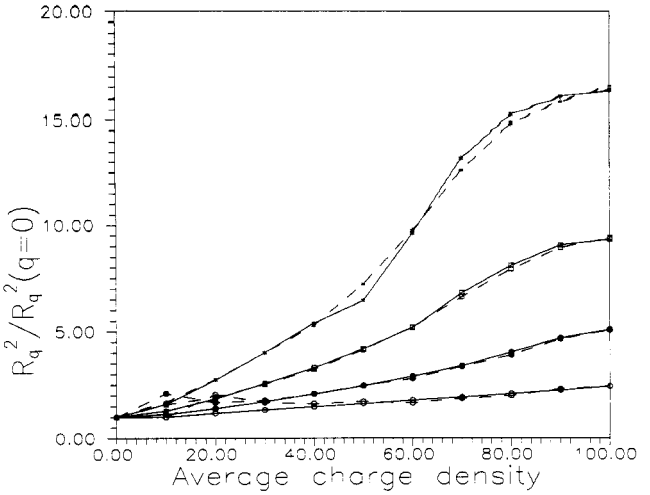

Figure 4. Normalized squared radius of gyration of the charges: $R_q^2/R_q^2(q=0)$, versus the average charge density, for chains of 10 (○), 20 (●), 40 (□), and 80 (*) segments with either mobile (—) or equidistantly fixed (- - -) charges. $\kappa a = 0.1$.

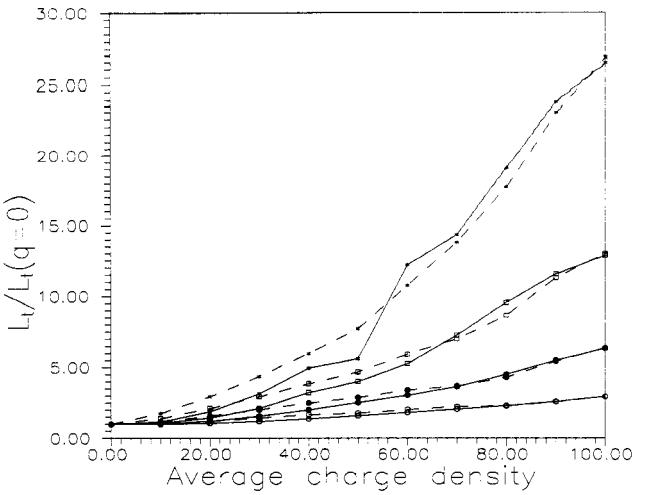

Figure 5. Normalized average projection of the end-to-end vector on the first step: $L_t/L_t(q=0)$ versus the average charge density, for chains of 10 (○), 20 (●), 40 (□), and 80 (*) segments with either mobile (—) or equidistantly fixed (- - -) charges. $\kappa a = 0.1$.

$\kappa a = 0.1$ and for $n = 10$, 20, 40, and 80, for both mobile and fixed charges. For short chains and low charge density, $R_{q,\text{fixed}}$ is seen to be considerably larger than $R_{q,\text{mobile}}$. This is an artefact which results from positioning the charges equidistantly (e.g. for $q = 2$, the charges are placed at the end points). For charge densities between 20% and 50% the behavior of $R_{q,\text{mobile}}$ is similar to the behavior of $R_{q,\text{fixed}}$, whereas for larger charge densities there is a crossover to a region where $R_{q,\text{mobile}}$ is larger than $R_{q,\text{fixed}}$. The reason for this behavior is the charge accumulation near the end points. In the calculation of R_q the charge of a segment serves as a weight factor, which puts more emphasis on the ends of the chain. This behavior makes $R_{q,\text{mobile}}$ larger than $R_{q,\text{fixed}}$, at sufficiently high charge densities. Notice, that for a 100% charge density both values are again equal (within the accuracy). One may also compare $R_{q,\text{fixed}}$ and $R_{g,\text{fixed}}$. If the chains are not too short, and the charge density is not too low, these quantities are equal (within the accuracy) as one would expect. For a smaller charge density $R_{q,\text{fixed}}$ becomes larger than $R_{g,\text{fixed}}$, indicating that there is a sufficient distance between subsequent charges to position them on the average further away from the center of mass. In the mobile case this effect is more pronounced and $R_{q,\text{mobile}}$ is larger than $R_{g,\text{mobile}}$ for all charge densities. For $\kappa a = 2.0$ the differences between the fixed and mobile case are negligible, i.e. comparable with the estimated error of about 2% in the calculated results.

In Figure 5 the apparent persistence length, L_t (see eq 6), is plotted as a function of the charge density, for $\kappa a = 0.1$ and for $n = 10$, 20, 40, and 80, for fixed as well as for mobile charges. In this case one sees that for small charge densities the $L_{t,\text{mobile}}$ is smaller than $L_{t,\text{fixed}}$, whereas for large charge densities this is the other way around. For increasing chain length the crossover shifts to a lower value of the charge density. As we discussed in connection with Figure 3, the charge mobility enhances the flexibility of the chain, which causes $L_{t,\text{mobile}}$ to be smaller than $L_{t,\text{fixed}}$ as long as the charge density is not too high. At higher charge densities the enhancement of the flexibility due to the charge mobility becomes relatively less important as a consequence of the lack of open places. In this case the charge accumulation near the end points again plays a dominant role. This charge accumulation stiffens the chain near the ends, and as L_t measures in particular the stiffness near the ends of the chain, $L_{t,\text{mobile}}$ then becomes larger than $L_{t,\text{fixed}}$. Notice the fact that in the rest of the chain the average charge density decreases slightly, due

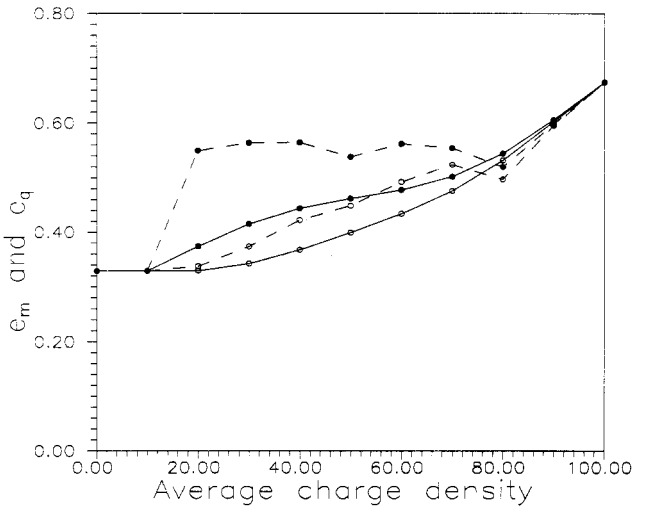

Figure 6. Eccentricity of the mass (○) and the charge (●) distribution, versus the average charge density, for a chain of 10 segments with either mobile (—) or equidistantly fixed (- - -) charges. $\kappa a = 0.1$.

to the charge mobility, so that there the flexibility is even more enhanced. While this is not important for L_t, it is important for R_g, and as a consequence one does not find a similar crossover for R_g. In the limit of zero charge density L_t reduces to $L_t(q=0)$, which is almost independent of the chain length, and has a value of about $1.42a$. In the limit of a 100% charge density we find that L_t becomes proportional to the chain length. For $\kappa a = 2.0$ the differences between the fixed and mobile cases are again very small.

In Figures 6 and 7 the eccentricities of the mass and charge distributions are plotted for $\kappa a = 0.1$, for chains of 10 and 40 segments. These plots show that the eccentricities decrease as a function of the chain length. This decrease is also a function of the charge density. For zero charge density the eccentricities are found to be inversely proportional to the chain length. For increasing charge density this dependence becomes less pronounced, until, at the maximum charge density, the eccentricities are found to be independent of the chain length. Around a charge density of about 65% there is a crossover. Below this crossover the eccentricities for the fixed-charge distribution are larger than the corresponding eccentricities of the mobile case. Above the crossover the situation is reversed. Furthermore, the eccentricities of the mass

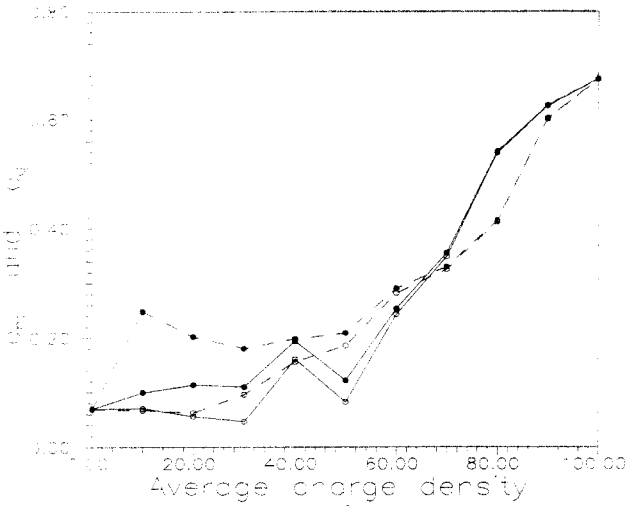

Figure 7. Eccentricity of the mass (O) and the charge (●) distribution, versus the average charge density, for a chain of 40 segments with either mobile (—) or equidistantly fixed (- - -) charges. $\kappa a = 0.1$.

and charge distribution become practically identical above the threshold. The relatively large eccentricity of the charge distribution for fixed charges at a low charge density is again an artefact of the position of the charges at the end points of the chain. For increasing chain length this effect disappears. For $\kappa a = 2.0$ the differences between the fixed and mobile cases are again negligible.

For increasing values of κa, which implies a more effective screening of the polyion charges, electrostatic effects are suppressed to a high degree. Qualitatively, however, all results show, though to a lesser extent, the same general trends. In particular the differences between the fixed and mobile-charge cases again find their origin in a more uniform average charge distribution, in the mobile case, as well as a charge accumulation near the end points. We will not elaborate upon this point any further.

4. Influence of Charge Mobility

The differences between both (fixed and mobile charged) cases are primarily induced by a more uniform average charge distribution in the mobile case and a charge accumulation of the mobile charges near the ends of the chain. This causes the chain with mobile charges to be more flexible in the middle part, and more stiffened at the ends, in comparison to the chain bearing equidistantly fixed charges. Furthermore, the mobile charges will tend to preferentially localize themselves away from bends in the chain, thus enhancing its flexibility. The effect of the charge mobility is most important at charge densities of about 50%.

In general, chain dimensions expand upon charging the chain. But the middle part of the chain with mobile charges will not swell as much as it would if its charges were fixed, as a result of the redistribution of charge away from bends and toward the chain's end points. On the other hand, the ends protrude more outward, as the repelling electrostatic forces between the bulk of the chain and the end points are stronger in the mobile case, provided that the charge density is high enough for this charge accumulation to be important, compared to the charges present at the end points in the fixed case. This effect leads to a higher eccentricity of both the mass and charge distributions in the mobile case, but its net effect on the end-to-end distance and both radii of gyration is relatively small: the stiffness of the ends and the less-swollen middle part of the chain compensate, surprisingly, each others influence on these more global properties of the chain to a large extent. But not quite, as the differences, for instance between $R_{g,mobile}$ and $R_{g,fixed}$ (and this is also true for the corresponding R_q and R_e), do indeed increase at increasing chain length, although relatively slowly, for the lengths considered in this paper. In the limit of really long chains one generally expects end effects to disappear. Consequently, the higher flexibility of the middle part of the chain with mobile charges is less compensated by the stiffened ends in the long-chain limit, so that the slow increase of this difference is expected to persist. Calculations involving longer chains might be more conclusive in this respect.

At lower charge densities and especially for short chains, the fixed charges at the end points play such a dominant role that there the eccentricity of the charge distribution is much larger than in the mobile case. There is even a relatively large effect on R_q. This, however, must be considered an artefact, resulting mainly from the way in which the fixed charge distribution is chosen.

Whether the charges are fixed or not, (the eccentricities of) the mass and charge distributions show obvious differences, provided the charge density is not too high. In both the fixed and the mobile cases the charge distribution is less spherical than the mass distribution, an effect which is a bit suppressed by charge mobility. Differences are less clearly visible in the behavior of more global properties (like, e.g., the charge and mass radius of gyration). As one would expect, the charges distribute themselves, on the average, slightly further away from the center (of mass) than the mass itself, which is reflected in the fact that R_q is always a bit larger than R_g. The effect of charge mobility is of less importance here.

5. Comparison with Theory

Many polyelectrolyte theories have been devoted to polyion expansion. Hence, it should be of interest to compare the predictions of the expansion behavior emerging from our model with those from other approaches. Obviously, we have to restrict ourselves to an isolated, charged chain, immersed in a salt environment, ignoring polyion–polyion interactions which in reality may be present at low salt, and especially at higher polyion, concentrations.

In particular we shall consider the expansion of a charged chain of 80 segments, as a function of increasing charge density (see Figure 3) at two different salt concentrations ($\kappa a = 0.1$ and $\kappa a = 2.0$). From a theoretical point of view, the comparison is most adequately made by using the end-to-end distance R_e, instead of the radius of gyration R_g.

One of the first attempts to describe polyion expansion is due to Katchalsky et al.[16,17] In this approach, shortly outlined by eqs A.1–A.6 in the Appendix, the end-to-end distance of the charged chain is found by minimizing the sum of an elastic and an electrostatic free energy. Both parts are based on the statistics of a Gaussian chain, whereas for the electrostatic interaction a screened Debye–Hückel potential has been used. This theory is known to overestimate the expansion of polyelectrolytes. More realistic models were proposed later on, but they remain more or less as unsatisfactory. Most of them have been reviewed in the book by Morawetz[24] and are not considered here.

Some of the failure of Katchalsky's theory can be eliminated by calculating the elastic part of the free energy from the statistics of the wormlike chain. This route has been followed recently by Schmidt et al.[18,19] In this model the total free energy depends on the contour length L and

the total persistence length L_p and is minimized with respect to the latter. The resulting value of L_p can be inserted into the expressions for the end-to-end distance and the apparent persistence length of a wormlike chain. In (A.7)–(A.12) and (A.17) in the Appendix, further details of this calculation are presented.

A more explicit way to obtain the apparent persistence length L_t, is to calculate first the electrostatic part L_e of the (regular) persistence length, according to the theories of Odijk[4] and of Skolnick and Fixman.[12] Both Odijk and Skolnick consider the continuously charged wormlike chain (to which we will refer as "Odijk's model"). Skolnick also considers a wormlike chain with a discrete, equidistant charge distribution ("Skolnick's model"), as well as mobility and fluctuations in the continuous charge distribution. In the latter two cases the authors restrict themselves to charge variations over distances large compared to the Debye length. They find that such variations are unimportant. In our analysis we find that charge variations on a shorter length scale play the more important role in the properties of the chain.

In its most general form, L_e is given in the Appendix, by eqs A.14 and A.15 for Odijk's model and by (A.16) for Skolnick's model. These equations show the explicit dependence of L_e on the charge density and the salt concentration. Once L_0 is known, the total persistence length L_p is found by using eq 8. Then the polyion expansion can be described as before, with the end-to-end distance of the wormlike chain, given in eq A.13, and the apparent persistence length (from (A.17)) both as a function of varying L_p.

In the above approaches, the excluded volume interaction between chain segments has not been taken into account, i.e. the chain may intersect itself. This will certainly not be realistic at high values of κa, where the charged chain is still more or less coiled, making situations of close approach between different segments frequent. Following Odijk, we can include the excluded volume effect in the theoretical description, at least for a charged chain with a sufficiently large number of Kuhn statistical segments. In (A.17)–(A.20) in the Appendix, the explicit formulas to include this effect are presented.

Finally, we compare our MC calculations with another MC model, recently reported by Carnie et al.[6] In the cited model the chain consists of spherical, charged beads connected with bonds of length 0.252 nm (identical to our step length a), making a bond angle of 109.5°. The beads interact with each other by means of a Debye–Hückel potential of mean force, like in our model, superimposed on a repulsive hard sphere interaction, which leads to self-avoiding walk statistics, as in our MC calculations. The bonds are allowed to rotate freely. However, hindered rotation with a preference for gauche and trans conformations is easily introduced in these simulations.[6]

In Figures 8 and 9 the expansion of the chain with increasing charge density is shown, according to the various theoretical predictions. The ratio of R_e^2 to its maximum value at full extension has been chosen, which describes most appropriately the relative expansion of the various models, in particular for higher charge densities and low κa. The limiting value of R_e^2 at full extension is defined to be the squared contour length L^2. For the models in which the chain may be stretched ultimately to a rod (i.e. Katchalsky, Schmidt, Odijk, Skolnick, and this paper) L is equal to $79a$, being the contour length of a chain of 80 segments in our MC calculations. In the MC model of Carnie et al. the limiting stretched conformation is a zigzag chain, for which L becomes equal to[6] $79a \sin(109.5°/2)$. In

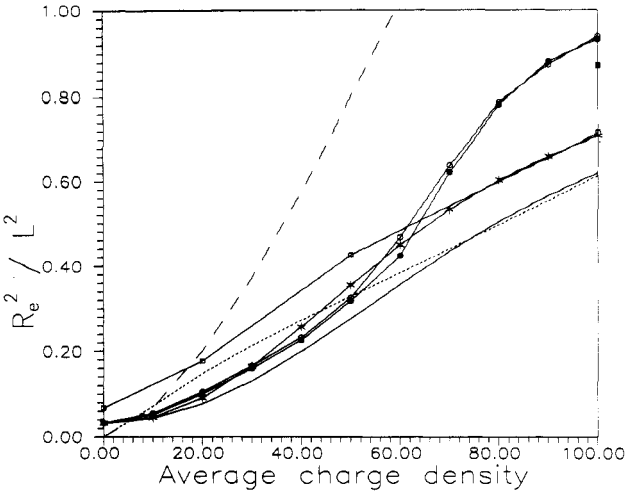

Figure 8. Squared end-to-end distance of a chain of 80 segments, normalized by its squared maximum extension, versus the average charge density, as predicted by various models for $\kappa a = 0.1$. Our results for mobile (●) as well as equidistantly fixed (○) charges are compared to predictions of Odijk (—), Skolnick (*), Katchalsky (- - -), and Schmidt (···) and simulation results of Carnie, Christos, and Creamer for freely rotating segment bonds (□) and chains with hindered rotation (■).

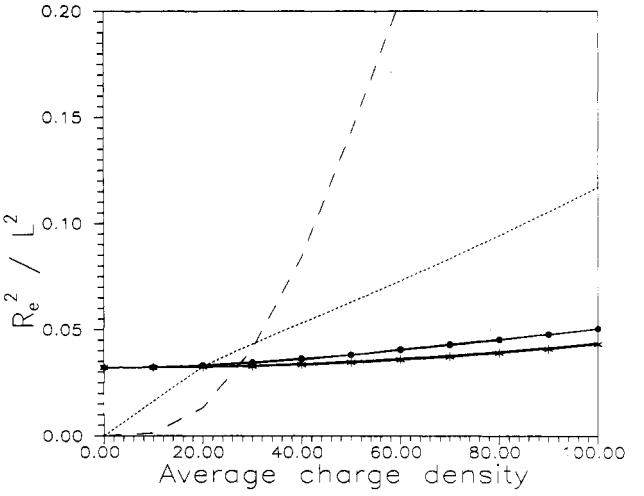

Figure 9. Squared end-to-end distance of a chain of 80 segments, normalized by its squared maximum extension, versus the average charge density, as predicted by various models for $\kappa a = 2.0$. Our results for mobile (●) as well as equidistantly fixed (○) charges (practically indistinguishable from each other) are compared to predictions of Odijk (—), Skolnick (*), Katchalsky (- - -), and Schmidt (···).

our use of Odijk's and Skolnick's models, the value of L_0 was chosen such that the resulting value of R_0 from the wormlike chain matches the value found in our MC calculation. For the Katchalsky model $R_0^2 = 79a^2$.

At $\kappa a = 0.1$ the screening of the charges on the chain is relatively low, and the chain expansion with increasing charge turns out to be strong (see Figure 8). In spite of the discrepancies existing among the different models, a common feature is observed in the occurrence of S-shaped curves in the MC models and Odijk's and Skolnick's models. This behavior is in conformity with what is to be expected in view of the finiteness of the chain length. In the curve of Schmidt such a typical S-shape is not seen. The difference between the results of the two MC models is a consequence of the fact that both models differ in the description of the local stiffness of the chain. This is nicely illustrated by the fact that introduction of hindered rotation in the model of Carnie et al. leads to a much better agreement between both MC results (see the single

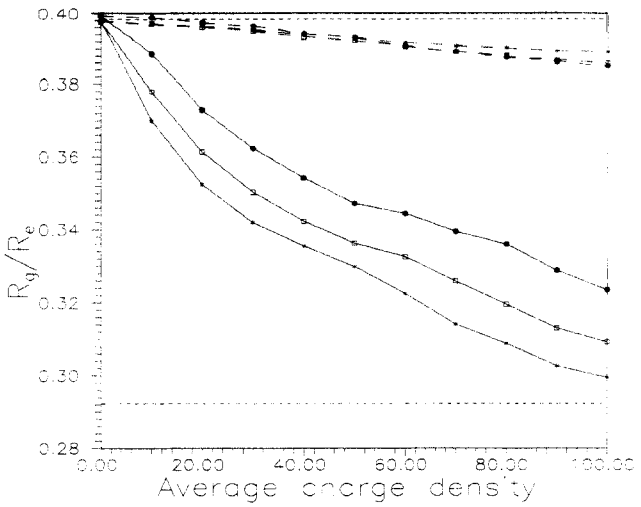

Figure 10. Ratio of the radius of gyration and the end-to-end distance R_g/R_e for chains of 20 (●), 40 (□), and 80 (*) segments versus the average charge density, for fixed charges, both for κa = 0.1 (—) and for κa = 2.0 (- - -). The upper dotted line is the prediction of des Cloizeaux for uncharged self-avoiding walks; the lower dotted line represents the rod limit.

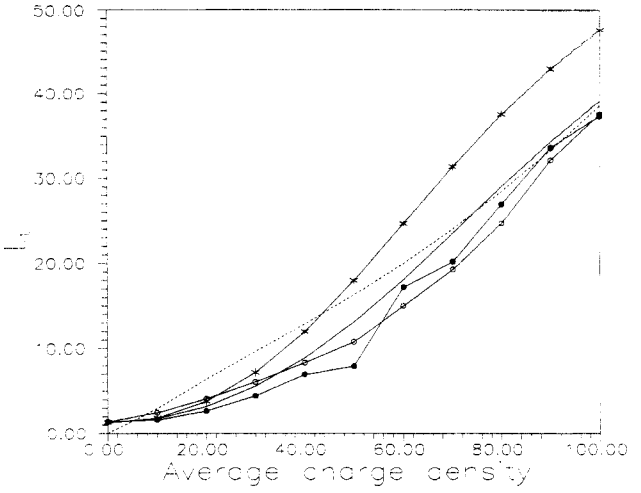

Figure 11. Length dependent persistence length L_t of a chain of 80 segments, versus the average charge density, with κa = 0.1, found for mobile (●) as well as equidistantly fixed (○) charges. For comparison the predictions by Odijk (—), Skolnick (*), and Schmidt (···) are also given.

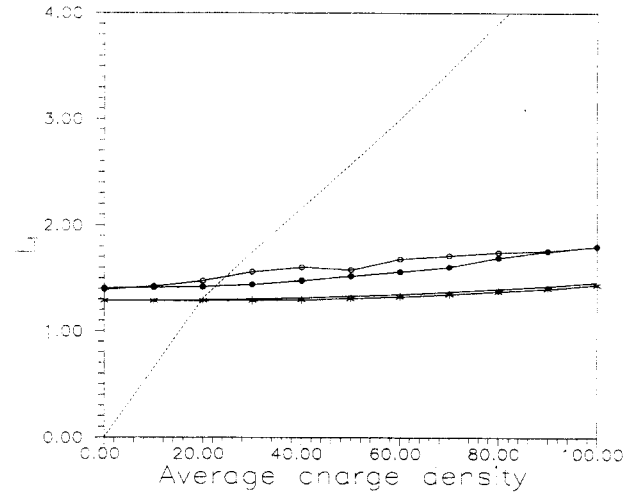

Figure 12. Length dependent persistence length L_t of a chain of 80 segments, versus the average charge density, with κa = 2.0, found for mobile (●) as well as equidistantly fixed (○) charges. For comparison the predictions by Odijk (—), Skolnick (*), and Schmidt (···) are also given.

point in Figure 8). The rather rapid unfolding of the chain, observed in our simulations at relatively high charge density, is due to a large contribution of conformations in which the middle part of the chain is already rodlike and bending occurs only near the ends. This is the reason that L_t is indeed much smaller than the value of the (ordinary) persistence length, L_p, estimated from Figure 8. On the contrary, the expansion found by Carnie et al. follows more the wormlike chain models of Odijk, Skolnick, and Schmidt. This is mainly due to the fact that their model allows more smooth changes in conformation than ours. Skolnick's wormlike chain with a discrete charge distribution gives a somewhat better value for the end-to-end distance than Odijk's wormlike chain with a continuous charge distribution.

Katchalsky's results overestimate considerably the chain expansion in a region where the predictions of the other theories globally overlap (see Figure 8 with the charge density between 20% and 60%). Obviously, the main reason is that many conformations in which the chain intersects itself are erroneously counted in ΔF_{electr}, thereby enlarging the repulsive contributions in an unrealistic way. Thus the expansion starts with a driving force which is much too high. In this respect the model of Schmidt, where the statistics of the wormlike chain are used instead of those of the Gaussian chain, seems to be better, as less intersections of chain segments are allowed to occur.

When the screening of the charges is more complete (κa = 2.0, the results are shown in Figure 9), the chain expansion with charge density is rather suppressed, as expected. Again it is seen that the approach according to Katchalsky's model exaggerates the chain expansion. To a lesser degree this also applies to the prediction of Schmidt's model, as the number of intersections of the wormlike chain also becomes important at this value of κa.

Figure 10 shows how the chain changes from the coil-like limit in the uncharged state to a more rodlike form when the fixed-charge density is increased. The behavior for mobile charges turns out to be almost the same (not shown). For a swollen, uncharged coil (including the excluded-volume effect) R_g/R_e has been estimated[25] to be equal to $(1/6.302)^{1/2}$, whereas for a completely stretched chain we find R_g/R_e = 0.2923, almost equal to $(1/12)^{1/2}$, expected for a homogeneous rod. Both limits are indicated in Figure 10. Our simulations predict that at κa = 0.1 the form of the chain changes from coil-like to almost rodlike. Notice also the dependence of the chain length. On the other hand it is found that at κa = 2.0 the chain retains almost completely its coil-like character.

In Figure 11 the apparent persistence length, L_t, has been plotted as a function of the charge density, for the chain of 80 segments with κa = 0.1. The difference between the mobile and the fixed-charge case has been discussed already in section 3. The curves according to the theories by Odijk, Skolnick, and Schmidt are also given. For low charge densities Odijk's and Skolnick's values are in better agreement with the numerical results than Schmidt's values, which are somewhat too high. For high charge densities Skolnick's values are considerably higher than the other theories, that converge more or less. For κa = 2.0 (cf. Figure 12) both the numerical and the Odijk and Skolnick values are almost independent of the charge density. The discrepancy is a consequence of the choice of L_0, which persists for all values of q, as the electrostatic contribution to L_t is small for large κa. Our choice of L_0 gives a correct value for R_e^2 at q = 0. The above discrepancy originates from the difference between the lattice chain

and the wormlike chain and is therefore somewhat artificial. Schmidt's values are strongly dependent on the charge density and are therefore in both qualitative and quantitative disagreement with the numerical results.

6. Conclusions

Although there is an effect of charge mobility on global properties of the chain (e.g. R_e, R_g, R_q), which effect becomes slightly more important at increasing chain length, the effect on properties that depend strongly on the local stiffness of the chain (e.g. L_t, eccentricities) is especially more manifest. So, in particular when quantities of the latter kind are studied, charge mobility, when it may occur, should explicitly be taken into account. The observed differences in behavior owing to the mobility of charges are ascribed to a more uniform average charge distribution in the mobile case and a charge accumulation of the mobile charges near the ends of the chain. Furthermore, the mobile charges will tend to preferentially localize themselves away from bends in the chain, thus enhancing the flexibility of the chain. The resulting effects are most pronounced for small κa but are to a lesser extent still present at larger values of κa.

With regard to the mass and charge distribution we find that the eccentricity of the charge distribution is larger than the eccentricity of the mass distribution, which effect is most prominently seen in the case of fixed charges and at low values of κa.

If one compares our numerical results with theoretical predictions, one finds that Katchalsky's theory grossly overestimates the expansion of the polyelectrolyte. For large κa Schmidt's theory is in poor qualitative and quantitative agreement with our MC results, both regarding the expansion and the apparent persistence length. For small κa the agreement is much better. Both Odijk's and Skolnick's theories agree qualitatively with our numerical results. The quantitative agreement is much poorer. The remaining discrepancies between our MC calculations and all theories are caused by the fact that the simulation is performed for a lattice polyelectrolyte, while the theory uses a wormlike chain. The lattice chain expands more strongly, due to the incorporated hindered rotation. This effect is in particular strong for a large charge density and small values of κa. Similar findings emerge also from the calculations of Carnie et al.[6]

Appendix

Approach of Katchalsky et al.[16,17] The electrostatic free energy is calculated by averaging the Debye–Hückel interactions between the charges on all segment pairs, over all possible chain conformations, at a fixed end-to-end distance of a Gaussian chain.

The resulting integral expression for the electrostatic free energy is

$$\Delta F_{\text{electr}}(R) = \int_{\xi=0}^{1} d\xi\,(1-\xi) \int_{r=0}^{\infty} dr\, \frac{1}{2}\left\{\frac{q^2 e^2}{4\pi\epsilon r}\right\} e^{-\kappa r} W(\xi,r,R) \tag{A.1}$$

In this expression

$$W(\xi,r,R) = [\pi h_0{}^2 \xi(1-\xi)]^{-1/2} \frac{r}{\xi R}\left\{\exp\left[-\frac{(r-R\xi)^2}{h_0{}^2\xi(1-\xi)}\right] - \exp\left[-\frac{(r+R\xi)^2}{h_0{}^2\xi(1-\xi)}\right]\right\} \tag{A.2}$$

is the probability density of finding two segments, separated a distance ξL along the contour, at a spatial distance r, while the chain is being held at a fixed end-to-end distance R. Furthermore, $h_0{}^2$ ($=^2/_3 R_0{}^2$) is the square of the *most probable* end-to-end distance of the uncharged chain, its average end-to-end distance being $R_0{}^2$.

The integral in eq A.1 can be evaluated at $\kappa = 0$ and gives

$$\Delta F_{\text{electr}}(R) = q^2 \frac{Q}{R} kT\left[1 + \ln\left(\frac{3R^2}{2R_0{}^2}\right)\right] \tag{A.3}$$

At medium ionic strength, (A.1) is approximated by

$$\Delta F_{\text{electr}}(R) = q^2 \frac{Q}{R} kT \ln\left[1 + \frac{6R}{\kappa R_0{}^2}\right] \tag{A.4}$$

For the elastic contribution to the free energy, Katchalsky uses the leading order term of the entropy at a fixed end-to-end distance of a Gaussian chain:

$$\Delta F_{\text{elastic}}(R) = \frac{3}{2} kT\left(\left[\frac{R}{R_0}\right]^2 - 1\right) \tag{A.5}$$

The total free energy of the chain is now taken as a simple sum of both contributions:

$$\Delta F(R) = \Delta F_{\text{electr}}(R) + \Delta F_{\text{elastic}}(R) \tag{A.6}$$

Finally, R can be calculated numerically, by minimization of $\Delta F(R)$ with respect to R.

Method of Schmidt et al.[18,19] For the end point distribution of the bare chain an expression for the wormlike chain without excluded volume, derived by Koyama,[20] is used, instead of the corresponding one for a Gaussian chain.

$$4\pi R^2 W(R,L) = \frac{R}{2AB\sqrt{\pi}}\left\{\exp\left[-\left(\frac{R-B}{2A}\right)^2\right] - \exp\left[-\left(\frac{R+B}{2A}\right)^2\right]\right\} \tag{A.7}$$

where $A^2 = \langle R^2\rangle(1-y)/6$, $B^2 = y\langle R^2\rangle$, and $2y^2 = 5 - 3\langle R^4\rangle/\langle R^2\rangle^2$, in which both averages, $\langle R^2\rangle$ and $\langle R^4\rangle$, are well-known functions of L and L_p in the wormlike chain model (see p 53 of ref 22).

The elastic contribution to the free energy is in a first order approximation given by

$$\Delta F_{\text{elastic}}(L,L_p) = -T\Delta S = -kT\int_0^\infty 4\pi R^2 \{W(R,L) - W_0(R,L)\} \ln(W_0(R,L))\, dR \tag{A.8}$$

where W_0 denotes the end-to-end distribution of the uncharged chain (with bare persistence length L_0) and W the end-to-end distribution of the charged chain (with persistence length $L_p = L_0 + L_e$).

The average Debye–Hückel potential between two charges separated by a spatial distance r and contour distance s, is given by

$$\phi_{\text{cou}}(s) = QkT\int_0^\infty 4\pi r^2 \frac{e^{-\kappa r}}{r} W(r,s)\, dr \tag{A.9}$$

$$= QkT\frac{e^{\kappa^2 A^2}}{2B}\{e^{-\kappa B}\,\text{erfc}(\kappa A - B/2A) - e^{\kappa B}\,\text{erfc}(\kappa A + B/2A)\} \tag{A.10}$$

in which A and B are defined as before, but with R replaced by r.

The electrostatic part of the free energy is then obtained by summing the average interaction potentials ϕ_{cou} over all possible charge pairs.

$$\Delta F_{electr}(L,L_p) = \sum_{k=1}^{q-1}(q-k)\phi_{cou}\left(\frac{kL}{q-1}\right) \quad (A.11)$$

where q is the total number of charges. The summation over k in this expression corresponds to the integral over ξ in Katchalsky's work (see eq A.1); the factor q - k, counting the number of charge pairs at a distance $kL/(q-1)$ along the chain, corresponds to the factor $(1-\xi)$. The total free energy of the chain reads

$$\Delta F(L_p) = \Delta F_{elastic}(L_p) + \Delta F_{electr}(L_p) \quad (A.12)$$

in which L_p now appears as the relevant minimization variable. Values of $\langle R^2\rangle$ are then obtained, within the model of the wormlike chain,[22] using (A.13).

$$\langle R^2\rangle = 2LL_p - 2L_p^2[1-\exp(-L/L_p)] \quad (A.13)$$

Electrostatic Persistence Length and the Wormlike Chain.[4,12] By taking into account only slightly bent, semicircular conformations of the polyion and the electrostatic interaction energies in a lowest order approximation, the electrostatic persistence length for a continuous charge distribution has been derived[4] as

$$L_e = \frac{1}{12}Qq^2h(\kappa L) \xrightarrow{\kappa L \to \infty} L_e = \frac{Qq^2}{4\kappa^2L^2} \quad (A.14)$$

where

$$h(x) \equiv e^{-x}\left(\frac{1}{x}+\frac{5}{x^2}+\frac{8}{x^3}\right)+\frac{3}{x^2}-\frac{8}{x^3} \quad (A.15)$$

For a discrete charge distribution, which corresponds to the case of equidistantly fixed charges, it is found[12] that

$$L_e = \frac{Q}{12}\left\{\frac{(1+\kappa A)e^{-\kappa A}}{(1-e^{-\kappa A})^2}+\frac{2\kappa Ae^{-2\kappa A}}{(1-e^{-\kappa A})^3}\right\} \quad (A.16)$$

where A $(=L/(q-1))$ is the distance between subsequent charges along the contour.

In a lowest order approximation, additivity of the bare persistence length L_0 and the electrostatic persistence length L_e can be adapted, i.e. $L_p = L_0 + L_e$ (see eq 8). Within the wormlike chain model the apparent persistence length, L_t, is related to the (infinite chain) persistence length, by

$$L_t = L_p[1-\exp(-L/L_p)] \quad (A.17)$$

Using eq 8 and (A.14) or (A.16), values of $\langle R^2\rangle$ and L_t can respectively be found by substituting the total persistence length L_p in (A.13) and (A.17). So far, these values do not contain yet the effect of the segmental excluded volume β.

Consider a chain consisting of a sufficiently large number of cylindrical Kuhn segments of length $2L_p$ $(L/2L_p \gg 1)$ and effective diameter d.[26] For the end-to-end distance, the excluded volume effect is expressed in terms of the expansion factor α_R. Thus, by definition

$$R_e^2 = \alpha_R^2(z)\langle R^2\rangle \quad (A.18)$$

where z represents the excluded-volume parameter, defined as

$$z = \left(\frac{3^{3/2}}{32\pi^{3/2}}\right)\beta L^{1/2}L_p^{-7/2} \quad (A.19)$$

For the calculation of α_R one may use Yamakawa's expression[22]

$$\alpha_R(z) = 0.572 + 0.428(1+6.23z)^{0.50} \quad (A.20)$$

Finally, β may be approximated by[12,26]

$$\beta = 2\pi L_p^2\left[\kappa^{-1}\left(\ln\left(\frac{4\pi}{Q\kappa}\right)+\gamma-\frac{1}{2}\right)+b\right] \quad (A.21)$$

in which b stands for a hard-core parameter, remaining when $q \to 0$ or $\kappa \to \infty$. According to (A.21), β has the form $2\pi L_p^2 d$, expected for cylindrical segments.

The above mentioned excluded volume correction is only valid when $L/2L_p \gg 1$, i.e. at relatively large values of κa.

Acknowledgment. The authors would like to thank M. Schmidt for an illuminating correspondence and T. Odijk for many fruitful discussions. One of the authors acknowledges support by the Koninklijke/Shell Laboratories, Amsterdam.

References and Notes

(1) Mandel, M. *Polyelectrolytes*; Encyclopedia of Polymer Science and Engineering, 2nd ed.; J. Wiley & Sons: New York 1988; Vol. 11.
(2) Fowler, R.; Guggenheim, E. A. Solutions of electrolytes. *Statistical Thermodynamics*, 2nd ed.; Cambridge University Press: Cambridge, U.K., 1956; Chapter 9.
(3) Valleau, J. P. *J. Chem. Phys.* **1989**, *129*, 163.
(4) Odijk, Th. J. *J. Polym. Sci., Polym. Phys. Ed.* **1977**, *15*, 477.
(5) Higgs, P. G.; Orland, H. *J. Chem. Phys.* **1991**, *95*, 4506.
(6) Carnie; Christos; Creamer. *J. Chem. Phys.* **1988**, *89*, 6484. Christos, G. A.; Carnie, S. L. *J. Chem. Phys.* **1989**, *91*, 439. Idem. *J. Chem. Phys.* **1990**, *92*, 7661.
(7) Brender, C.; Lax, M.; Windwer, S. *J. Chem. Phys.* **1981**, *74*, 2576. Idem. *J. Chem. Phys.* **1984**, *80*, 886.
(8) Manning, G. S. *J. Chem. Phys.* **1969**, *51*, 924.
(9) Skerjanč, J. *J. Chem. Phys.* **1990**, *93*, 6731.
(10) Khokhlov, A. *J. Phys. A* **1980**, *13*, 979.
(11) Fixman, M. *J. Chem. Phys.* **1990**, *92*, 6283.
(12) Skolnick, J.; Fixman, M. *Macromolecules* **1977**, *10*, 944.
(13) Domb, C. *Adv. Chem. Phys.* **1969**, *15*, 229.
(14) Metropolis, N. *J. Chem. Phys.* **1953**, *21*, 1087.
(15) Madras, N.; Sokal, A. D. *J. Stat. Phys.* **1988**, *50*, 109.
(16) Katchalsky, A. *J. Polym. Sci.* **1951**, *7*, 393.
(17) Katchalsky, A.; Lifson, S. *J. Polym. Sci.* **1953**, *11*, 409.
(18) Schmidt, M. *Macromolecules* **1991**, *24*, 5361.
(19) Förster, S.; Schmidt, M.; Antonietti, M. *J. Phys. Chem.* **1992**, *96*, 4008.
(20) Koyama, R. *J. Phys. Soc. Jpn.* **1973**, *34*, 1029.
(21) Flory, P. *Statistical Mechanics of Chain Molecules*; John Wiley & Sons, Inc.: New York, 1969.
(22) Yamakawa, H. *Modern theory of polymer solutions*; Harper & Row: New York, 1971.
(23) Le Bret, M.; Zimm, B. H. *Biopolymers* **1984**, *23*, 271.
(24) Morawetz, H. *Macromolecules in solution*, 2nd ed.; R. E. Krieger Publishing Co. Inc.: Malabar, FL, 1975.
(25) des Cloizeaux, J.; Jannink, G. *Les Polymères en Solution; leur Modélisation et leur Structure*; Editions de Physiques: Les Ulis, 1987.
(26) Odijk, T. *J. Biopolymers* **1979**, *18*, 3111.